Local and Global Response Parameters in Seismic Risk Assessment of RC Frames Retrofitted by BRBs

Fabio Freddi, Enrico Tubaldi, Andrea Dall'Asta
School of Architecture and Design, University of Camerino, Viale della Rimembranza, 63100, Ascoli Piceno, Italy.

Laura Ragni
Department of Civil and Building Engineering and Architecture, Polytechnic University of Marche, Via Brecce Bianche, 60131, Ancona, Italy.

ABSTRACT

This paper deals with the seismic performance and risk assessment of existing reinforced concrete (RC) buildings with limited ductility retrofitted by means of buckling restrained braces (BRBs). Two different approaches for evaluating the seismic vulnerability and risk before and after retrofit are introduced and analyzed. These approaches involve the use of different categories of engineering demand parameters (EDPs) for the system response assessment: global EDPs, that permit to obtain a synthetic description of the system behavior at a reduced computational cost, and local EDPs, more accurate in describing the response of the frame elements and of the BRBs, though more demanding from a computational point of view. The effect of the EDPs choice is analyzed by considering a two-dimensional RC frame designed for gravity-loads only as case study. The frame is retrofitted by introducing elasto-plastic dissipative braces designed for different levels of base shear capacity. The results of the study show that the use of global EDPs leads to a significant overestimation of the retrofit effectiveness in terms of both vulnerability and risk reduction. If a risk-based design is carried out for the retrofit system, braces with significantly lower dimensions are obtained by using global EDPs instead of local EDPs.

1 INTRODUCTION

The damage occurred during recent earthquakes in many existing reinforced concrete (RC) buildings designed before the introduction of modern seismic codes has shown that these structures are very vulnerable to the seismic action due to their reduced ductility capacity. Thus, there is a significant need of modern retrofit techniques for increasing their safety and of reliable tools for assessing the effectiveness of the retrofit.

Among the various techniques currently employed for the retrofit, the use of dissipative braces appears to be very promising (Soong and Spencer 2002). These braces provide a supplemental path for the earthquake induced horizontal actions and thus enhance the seismic behavior of the frame by adding dissipation capacity and, in some cases, stiffness to the bare frame. It should be noted, however, that the introduction of a bracing system into a low-ductility frame often induces remarkable changes both in the collapse modalities and in the probabilistic properties of the seismic response of the structure. The latter aspect assumes a considerable importance in consequence of the high degree of uncertainty affecting the seismic input and of the differences in the propagation of this uncertainty through the two resisting systems (RC frame and dissipative bracing). For these reasons, the evaluation of the effectiveness of this type of retrofit technique in reducing the frame vulnerability should be performed within a probabilistic framework.

A rational and widespread approach for assessing in probabilistic terms the seismic performance of a structural systems and the retrofit effectiveness involves the development of fragility curves. These tools provide the probability of exceeding a specified limit state

(LS) or failure condition, conditional to the strong-motion shaking severity, quantified by means of an appropriately selected intensity measure (*IM*). In this context, fragility curves are employed by Hueste and Bai 2006, Ramamoorthy et al. 2006, Güneyisi and Altay 2007, Özel and Güneyisi 2010. Although in these studies probabilistic methodologies are employed for evaluating the effectiveness of different retrofit schemes, some modifications and extensions should be introduced in order to properly address the specific issues deriving from the use of dissipative braces for the retrofit of existing low-ductility RC frames.

The first issue is related to the choice of appropriate engineering demand parameters (EDPs) for monitoring the seismic response and evaluating the performance of the frame and of the retrofit system. In the studies listed above the fragility curves are developed by using the peak interstory drift as unique global EDP. This strategy is commonly pursued since monitoring the time-history of the local response of all structural members may be cumbersome, especially when complex models with a high number of degrees of freedoms are considered. In the cases of existing structures designed before the introduction of modern seismic codes, the relationships between local failure and global EDPs, such as the interstory drift, may change case by case, as demonstrated by the very different drift limits present in the literature (Hueste and Bai 2006, Ramamoorthy et al. 2006). Moreover, in existing structures retrofitted by means of dissipative braces, these relationships could change by increasing the dimension of the braces, due to the reduction of the flexural ductility capacity of the compressed columns involved in the bracing system. For these reasons, the use of global EDPs with code-specified limits is not recommended for the assessment of existing RC frames. By contrast, the use of local component-specific EDPs (Lupoi et al. 2002), such as the strain demand at the most critical element sections or the shear demand on a beam-column joint, though more cumbersome, is not affected by the mentioned limitations. In addition, it permits to appropriately assess the probabilistic response of single resisting components (including the braces), their contribution to the system vulnerability, and the impact of the retrofit on the local response of the individual members (Padgett and Des Roches 2008).

A second relevant issue in defining a probabilistic methodology of analysis concerns the evaluation of the retrofit technique effectiveness, which is accomplished in the studies cited above by comparing the median values of the fragility curves of the structure before and after retrofit. This comparison has often implied the use of structural-independent *IM*s in past studies, such as the not very efficient peak ground acceleration (PGA). In fact, when the natural period of the bare frame differs from the natural period of the retrofitted frame, the comparison between fragility curves obtained by using more efficient structure-specific *IM*s (Katsanos et al. 2009) (e.g., the spectral acceleration at the fundamental period of the structure) would not directly provide information about the effectiveness of the retrofit (Liel et al. 2011). Furthermore, a more rational approach to accurately compute the changes in the safety margin due to retrofit should also account for the dispersion of the fragility curve, since this parameter affects the estimate of the seismic risk.

In Freddi et al. (2012), a probabilistic methodology aiming at overcoming the limits of the studies mentioned above is presented. The methodology is developed by combining existing techniques already employed for different structural systems and by tailoring these techniques to the specific problem analyzed. Local EDPs are used to develop single component fragility curves of a case study while system fragility curves are derived and described by proper synthetic parameters suitable for use with any *IM*. The retrofit effectiveness is evaluated by introducing proper synthetic parameters that allow the description and comparison of the fragility curves before and after the retrofit.

This paper aims at evaluating the effects of EDPs choice on the seismic risk assessment and risk-based design of the retrofit of existing RC frames by BRBs. For this purpose, the case study already studied in Freddi et al. (2012) is considered. This consists of an existing RC frame with low ductility capacity retrofitted by inserting a system of BRBs with elasto-plastic behavior designed for several levels of the base shear capacity. The braces are designed by applying a widespread method based on an equivalent single degree of freedom (SDOF) approximation (Soong and Spencer 2002). Fragility curves of the bare and of the retrofitted frame, built by considering local or global EDPs, are used to evaluate the seismic risk under different hazard scenarios. The comparison of the risk estimates sheds light on the effectiveness of the retrofit and on the effects of EDPs choice on the safety level achieved by the retrofit.

2 PROBABILISTIC METHODOLOGY FOR VULNERABILITY ASSESSMENT

This section introduces the probabilistic methodology proposed in Freddi et al. (2012) for the vulnerability assessment and retrofit effectiveness evaluation. The methodology takes into account the uncertainty affecting the earthquake input by considering a set of natural ground motion (g.m.) records that reflect the variability in duration, frequency content, and other characteristics of the input. The effects of model parameter uncertainty and epistemic uncertainty are usually less notable than the effects of record-to-record variability and they are not considered in this study (Kwon and Elnashai 2005).

In order to generate fragility curves, incremental dynamic analysis (IDA) (Vamvatsikos and Cornell 2002) is performed by subjecting the system to a set of selected g.m. records for increasing values of the seismic *IM*. The methodology proposed in this study is oriented to the use of structural-dependent *IM*s. In particular, the spectral acceleration $S_a(T)$ at the fundamental period of the structure T for a damping factor ξ=5% (Katsanos et al. 2009) is employed as *IM* due to its efficiency. This choice requires scaling the g.m. records in order to obtain the same value of $S_a(T)$ for the natural period of the structure, which is different for the bare and the retrofitted frames. IDA provides a set of samples of appropriately selected EDPs monitoring the system response for discrete values of the *IM*. As already discussed in the introduction, local EDPs, directly related to the component failure modes, are used in order to monitor the behavior of the most vulnerable system components and to capture the modifications to the frame response and collapse modalities induced by the introduction of the bracing system. The seismic demand on the frame elements (beams and columns) due to flexural moments and axial forces is controlled by monitoring the maximum-over-time values of the concrete compressive strain ε_c and of the steel strain ε_s at the most critical sections. The non-ductile mechanisms of the frames are controlled by recording the maximum-over-time values of the shear force V at the critical sections of each element of the frame, the diagonal tension stress σ_t, and the diagonal compression stress σ_c at each beam-column joint. Finally, in the retrofitted case, the seismic demand imposed on the retrofit system is controlled by evaluating the maximum-over-time value of a damage parameter i_d (e.g., the maximum-over-time value of the ductility

demand μ_d for elasto-plastic braces) for each dissipative brace. The component fragility curves for the bare and the retrofitted frame are evaluated by considering the following limit states (LSs) chosen coherently with the monitored EDPs: LS1) ε_c exceeding the capacity limit ε_{cu} at each critical section, LS2) ε_s exceeding the capacity limit ε_{su} at each critical section, LS3) the shear demand V exceeding the shear resistance V_u at each critical section, LS4) σ_c exceeding the resistance in compression σ_{cu} at each joint, LS5) σ_t exceeding the resistance in tension σ_{tu} at each joint, and LS6) the damage index i_d overcoming the corresponding capacity i_{du} at each dissipative brace, (e.g., μ_d overcoming the limit μ_{du} for elasto-plastic braces).

The system fragility curves are then derived by assuming a series arrangement of the components, i.e., failure in one component yields system failure. The choice of the LSs and the series arrangement assumption is consistent with seismic code prescriptions requiring that all the considered LSs must be verified for all the structural members. Moreover, it allows of limiting structural damage on the existing frame, often sought by the retrofit criteria. However, it is noteworthy that the proposed methodology can be applied also with different assumptions on the system fragility curves. Finally, it is noted that the proposed methodology is purely numerical since it is based on the direct comparison between the samples of the demand and the corresponding capacity. Thus, the correlation among the various component LSs is automatically taken into account. The numerical fragility curves are approximated by analytical lognormal curves obtained through least-square minimization. The assumption of lognormality simplifies the analysis of the results and permits to synthetically describe the fragility of the systems by means of the two characteristic parameters. These are the median fragility capacity, $IM_{c,50}$, defined as the 50th fractile of the lognormal fragility curve and the logarithmic standard deviation or dispersion measure, β_c, given by:

$$\beta_c = \frac{1}{2}\ln\left(\frac{IM_{c,84}}{IM_{c,16}}\right) \qquad (1)$$

where $IM_{c,84}$ and $IM_{c,16}$ are the *IM* values corresponding respectively to the 84th and the 16th fractile of the lognormal fragility curve, i.e., the values of the *IM* which yield failure respectively in 84 and 16 cases over 100. The use of lognormal fragility curves is very common and widely accepted in performance based earthquake engineering, since it permits to estimate the above

defined parameters even when a limited number of EDP samples are available. Moreover, it permits to easily incorporate the effects of other sources of uncertainty in addition to the record-to-record variability, and it simplifies the evaluation of the seismic risk.

As already pointed out in the introduction, if a structural-dependent IM such as $S_a(T)$ is employed to monitor the seismic intensity, the comparison of the values of $IM_{c,50}$ obtained for the bare and retrofitted frame would not directly provide information about the effectiveness of the retrofit, since the natural period changes due to the retrofit. For this reason, the comparison should be performed between the values of the "capacity margin ratio" m_{50} (Liel et al. 2011), defined as the ratio between the value of $IM_{c,50}$ and the value of the IM corresponding to a reference return period, IM_{TR}. In the proposed methodology, IM_{TR} is assumed as the value of $S_a(T)$ for a reference return period such that $m_{50}=1$ for the bare frame, as illustrated in Figure 1. By this way, the value of m_{50} obtained for the retrofitted frame directly measures the increment

of seismic intensity that can be withstood by the retrofitted structure. In a similar way, based on the ratio $IM_{c,84}/IM_{TR}$ and $IM_{c,16}/IM_{TR}$, the factors m_{84} and m_{16} corresponding to the 84th and 16th fractiles of increment of capacity are defined. These parameters, together with parameter β_c, may also be used to assess in probabilistic terms the effectiveness of the retrofit, by accounting for the dispersion of the system response, which may have a non-negligible influence on the seismic risk assessment.

Finally, it should be noted that the proposed methodology permits to draw some important considerations regarding the performance of the system before and after the retrofit. In fact, by directly comparing the single component fragility curves to each other and to the system fragility curve, it is possible to evaluate the most vulnerable components and their contribution to the system vulnerability. This comparison permits to understand the changes in the response and in the failure modalities of the frame due to the retrofit.
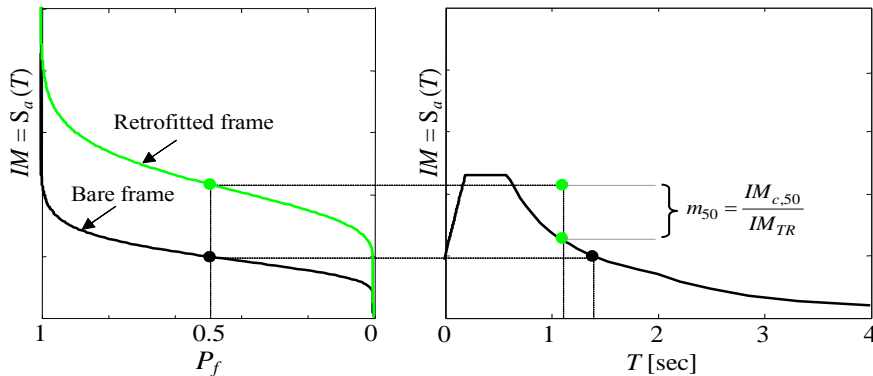

Figure 1. Definition of capacity margin ratio m50: seismic fragility curves before and after retrofit (left), uniform hazard spectrum such that m50=1 for the bare frame (right)

3 RETROFITTING OF RC FRAME WITH ELASTO-PLASTIC BRACES

A three story RC frame building is considered as case study. The building has been designed for gravity loads only and without any seismic detailing, applying the design rules existing before the introduction of modern seismic codes. The considered frame of the building is a three stories 3.66 m high and three bays, 5.49 m wide. Columns have a $300{\times}300$ mm^2 square section while beams are $230{\times}460$ mm^2 at each floor. Grade 40 steel ($f_y = 276$ MPa) and concrete with compression resistance $f_c' = 24$ MPa, were employed in the design. Figure 2 shows the general layout of the structure and the position of the braces. The complete detailing may be found in Bracci et al. 1995.
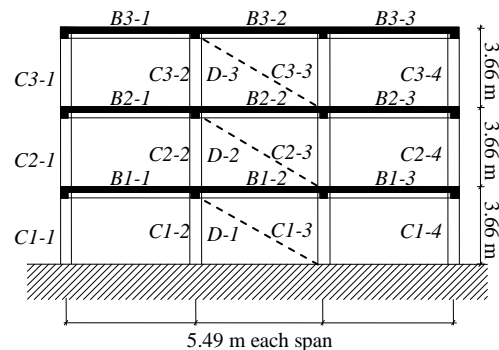

Figure 2. General layout of the structure and braces arrangement (adapted from Bracci et al. 1995).

A two-dimensional finite element (FE) model of the structure is developed in OpenSees (McKenna et al. 2006). Extended experimental results are available for a 1:3 reduced scale model of the frame and of its subassemblages (Bracci et al. 1995). The experimental information include

the results of quasi-static lateral load tests of columns and beam-column joint subassemblages and shaking table tests of the whole frame. The FE model is validated by comparing the experimental results with the simulated test results of the 1:3 scale numerical FE models showing good agreement at global and local scale.

The retrofit design method is based on the pushover analysis of the existing frame under a distribution of forces corresponding to its first vibration mode. The stiffness of the dissipative braces is distributed at each story ensuring that the first modal shape of the bare frame remains unvaried after the retrofit. The strength distribution of the dissipative braces aims at obtaining simultaneous yielding of the devices at all the stories in order to maintain a similar deformation also in the post-elastic range. The interested reader is referred to Dall'Asta et al. 2009 for a more detailed description.

Figure 3a shows the pushover curve obtained for the load distribution relative to the first vibration mode of the bare frame (mass participation factor of 86.4%). The ultimate capacity of the frame members is evaluated by considering the strain demand in the most critical concrete and steel fibres (ε_c and ε_s) and the corresponding limits $\varepsilon_{cu} = 0.0035$ and $\varepsilon_{su} = 0.04$ according to Eurocode 8. The other failure modes reported in Section 2 are not monitored in the application of the design procedure. The top story displacement $d = 0.102$ m denoting the failure of the most critical element (columns C1-2) is posed in evidence in Figure 3a. It corresponds to a

maximum interstory drift of about 1.0%, and to a base shear capacity $V^i_f = 186$ kN and it is assumed as the ultimate displacement d_u in the design procedure. Obviously, after this first failure, the bare frame still possess a residual capacity and can be pushed up to a top story displacement $d = 0.183$ m, at which all the base story columns fail (Figure 3c).

The dissipative devices adopted in this case are BRBs typically described by an elasto-plastic behavior (Zona and Dall'Asta 2012). Differently from those commonly used in steel-structures, the dissipative devices employed here are quite short, in order to obtain low yield displacements. Thus, the dissipative diagonal brace is made by assembling the BRB in series with an elastic brace characterized by an adequate over-strength. The ductility capacity μ_{0u} of the BRBs is assumed equal to 15, while the ductility capacity of the whole brace μ_{du} is assumed equal to 12 in order to obtain adequate dimension of the elastic braces. The bare frame is retrofitted by inserting a bracing system designed for several retrofit levels, measured by the ratio α between the base shear capacity of the bracing system V^I_d and that of the bare frame V^I_f. Parameter α assumes discrete values in the range from 0 (bare frame) to 3.2. Figure 3a reports the pushover curves for all the α values. In Table 1, the axial yield force F^i_d and elastic stiffness K^i_d of the dissipative braces are given for three retrofit levels considered. Table 1 also reports the fundamental vibration periods for each retrofit level considered, calculated by considering an effective stiffness of the RC frame elements.
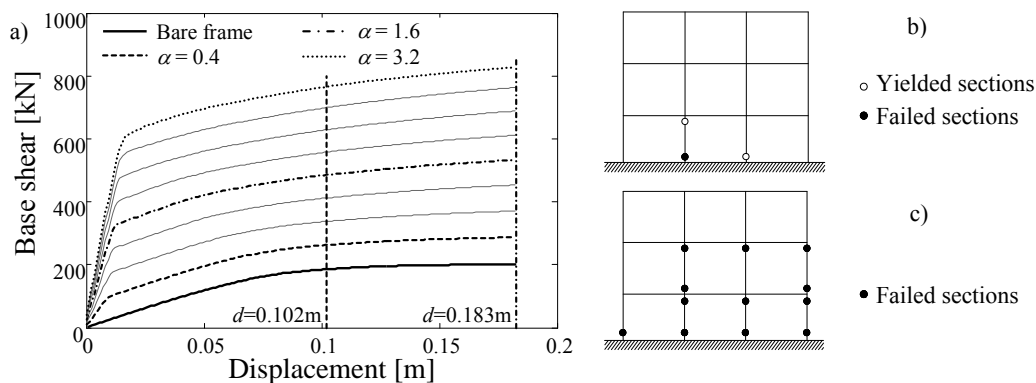

Figure 3. a) Pushover curves for bare and retrofitted frame, b) mapping of plastic hinges at d=0.102m , and c) mapping of plastic hinges at d=0.183m

Table 1. Dissipative braces properties at each story

	α=0.4 (T=0.670 sec)		α=1.6 (T=0.404 sec)		α=3.2 (T=0.321 sec)	
Story	F^i_d [kN]	K^i_d [kN/m]	F^i_d [kN]	K^i_d [kN/m]	F^i_d [kN]	K^i_d [kN/m]
1	88	36046	351	144183	702	288365
2	75	25106	301	100423	601	200847
3	43	22921	173	91685	346	183371

4 VULNERABILITY ASSESSMENT

For the purpose of developing fragility curves, a number of 30 natural g.m. records are selected from the European database. These records are chosen in a range of magnitude and source to site distance of 5.5-7.0 and 25-75 km respectively and are compatible with the type 1 hazard spectrum given in Eurocode 8, with soil type D ($S = 1.35$) and peak ground acceleration $a_g = 0.1S$g. In order to perform IDA, the records are scaled to the same value of the spectral acceleration at the fundamental vibration period of the system $S_a(T)$. It is noteworthy that the vibration period, and consequently the *IM* vary with α and thus, the g.m. records are re-scaled for each value of α. The dynamic analyses have been carried out on the numerical model developed in OpenSees and described in Section 3. For each record, for each *IM* value and for each element of the frame, the maximum-over-time values of the EDPs listed in Section 2 have been recorded. The maximum-over-time values of the tension (σ_t) and compression (σ_c) stresses and their capacity at each joints of the frame have been calculated through the formulas reported in Lupoi et al. 2002. Coherently with the capacity limits assumed in the retrofit design procedure, the limits of the concrete and steel capacity are set equal to $\varepsilon_{cu} = 0.0035$ and $\varepsilon_{su} = 0.04$, while the elements shear resistance V_u is evaluated according to the formulas reported in Lupoi et al. 2002. Figures 4 and 5 report the results of IDA, expressed in terms of variation with *IM* of the monitored EDP samples and their capacity. In Figure 4, the samples of the maximum-over-time values of the concrete compressive strain ε_c and steel strain ε_s at the most critical section of C1-2 are illustrated, for the case of the bare frame. The corresponding capacity limits are also reported. In the same figure, the values of σ_c and σ_t recorded at joint J1-1 are also reported and compared with the corresponding capacity limits. Figure 5 plots the values of ε_c at column C1-2 and the maximum-over-time value of the ductility μ_d experienced by dissipative brace D-1 at the base story, for the case of retrofitted frame with retrofit level α=1.6. The component fragility curves are evaluated for each LS and for each frame member by comparing the demand samples with the corresponding capacity limits. Then, the system fragility curves are derived by assuming a series arrangement of the component fragilities. Figure 6a reports the lognormal component fragility curves for the case of the bare frame. It is observed that joint failure in tension is the most critical LS. However, this LS provides only a measure of the damage of the joints due to the concrete degradation and it is not deemed as critical as the brittle failure of the joint in compression. Hence, it is disregarded in developing the system fragility curve and therefore concrete crushing in compression (LS1) is the most critical failure modality, while steel rupture (LS2) is much less probable and failure of joints in compression and shear failure have a zero probability of occurrence.
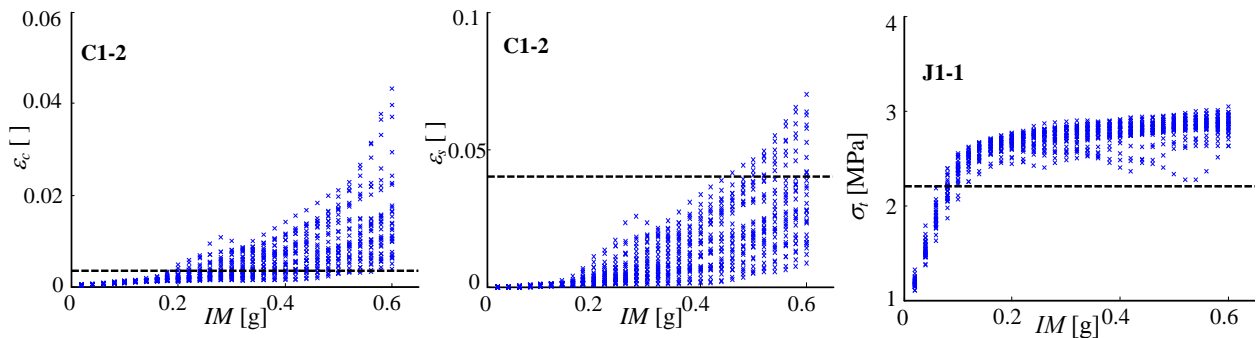

Figure 4. Demand samples and corresponding capacity limits for the case of bare frame
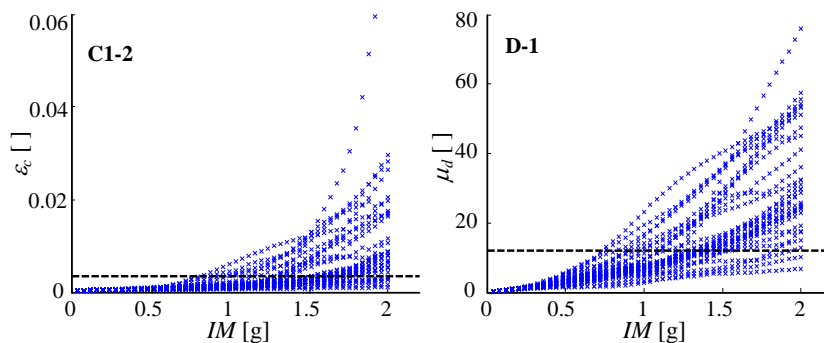

Figure 5. Demand samples and corresponding capacity limits for α=1.6

Figure 6b shows the fragility curves of the most vulnerable elements and of the system for three retrofitting levels corresponding to α=0.4, α=1.6 and α=3.2. The most vulnerable components of the bare frame are column C1-2 and C1-3, failing in concrete crushing mode (LS1) and exhibiting a similar vulnerability. For α=0.4 the vulnerabilities of the two columns remain comparable to each others, and also similar to the vulnerability of the most critical dissipative brace (D-1). This confirms the reliability of the simplified design procedure, which has the two main aims of avoiding drastic changes to the internal action distribution in the frame and of achieving a simultaneous failure of both the frame and the braces. Also in the case

corresponding to α=1.6, the fragility curves of the most critical frame components and of the most critical dissipative brace are very close. However, column C1-2 is more vulnerable than C1-3. This can be attributed to the bracing system configuration, which induces a higher axial load on column C1-2 with respect to C1-3. The trend is confirmed by the results of the case corresponding to α=3.2, where the fragility curve of column C1-2 differs significantly from the others and tends to coincide with the system fragility curve. This means that system failure is mainly due to C1-2 column failure, as consequence of the excessive axial force transmitted by the bracing system on this column.
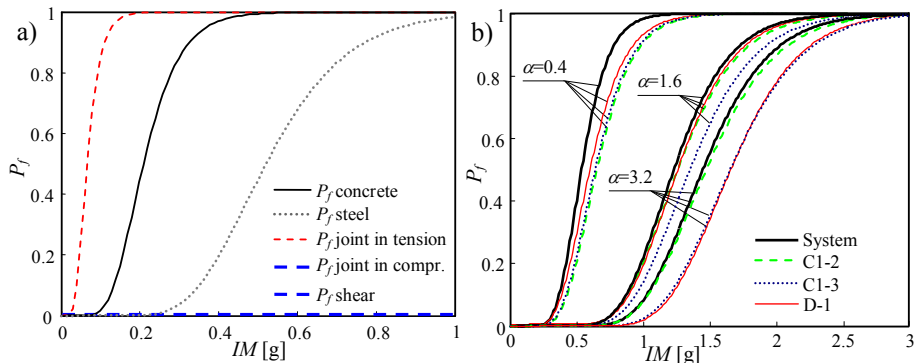

Figure 6. a) Lognormal fragility curves for the different failure modes and b) Fragility curve of the system and of the most vulnerable components for three retrofitted cases.
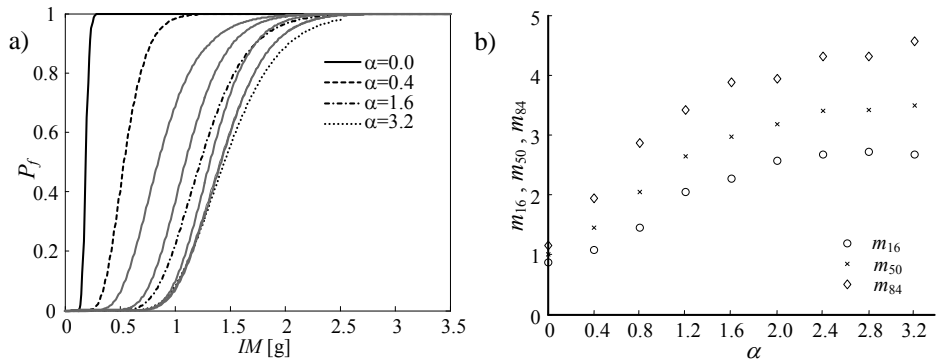

Figure 7. a) System fragility curves for the bare frame and for the retrofitted frame, and b) variation with α of factors m50, m84 and m16.
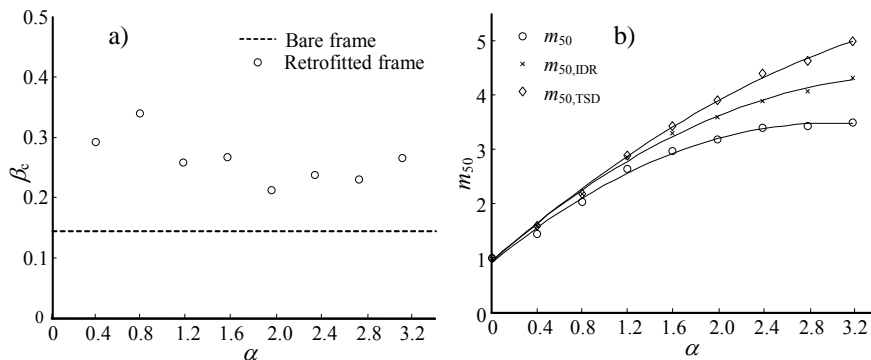

Figure 8. Variation with α of a) dispersion measure β_c and b) factor m_{50} corresponding to the use of different local and global EDPs.

Figure 7a compares the system fragility curves for all the retrofit levels considered. Parameter $IM_{c,50}$ increases for increasing values of α, as expected. However, as already stressed previously, this parameter does not directly provide information about the effectiveness of the retrofit, since the natural periods of the systems are different. Figure 7b reports the factors m_{50}, m_{84}, and m_{16}, which have been defined in Section 2 in order to compare the retrofit effectiveness when a structural dependent IM is used. It is observed that for values of α up to 1.6, the capacity margin ratio increases about linearly with α, while for higher values this relation becomes strongly non-linear. This implies that the effectiveness of the retrofit increases weakly for values of α larger than 1.6, in consequence of the premature failure of column C1-2 mainly due to the high axial forces induced by the braces.

Figure 8a plots the dispersion measure β_c evaluated according to Equation 1 for increasing values of α and shows that a significant increase of the dispersion occurs when elasto-plastic braces are introduced into the bare frame. This is consequence of the increase of the number of the vulnerable components (frame members and dissipative braces) and of the more pronounced nonlinear behavior induced by the introduction of BRBs. Accounting for this increase of dispersion is important due to its influence on the estimate of the seismic risk.

Finally, in order to quantify the differences in the retrofit effectiveness evaluation when local and global EDPs are used, system fragility curves are re-evaluated by considering global EDPs, such as the maximum interstory drift (IDR) and the top story drift (TSD). Figure 8b reports the comparison between the values of previously defined parameter m_{50} and the values of parameters $m_{50,\text{IDR}}$ and $m_{50,\text{TSD}}$ evaluated on the basis of the fragility curves developed by considering the IDR and the TSD respectively.

In order to make this comparison, the global EDPs limits IDR_u and TSD_u are chosen so that $IM_{c,50} = IM_{c,50;\text{IDR}}$ ($m_{50,\text{IDR}}=1$) and $IM_{c,50} = IM_{c,50;\text{TSD}}$ ($m_{50,\text{TSD}}=1$) for the case of bare frame. The limits obtained are $\text{IDR}_u= 1.302\%$ and $\text{TSD}_u= 1.029\%$. It is evident from Figure 8b that the use of global EDPs instead of more accurate local EDPs results in a significant overestimation of the seismic increment capacity of the retrofitted frames, especially for large α values. In fact, as already discussed in the introduction, local phenomena such as the increment of axial force in the columns adjacent to the dissipative braces are not accounted for by these global EDPs.

5   SEISMIC RISK ESTIMATE

Up to now, the study has quantified the effect of employing local rather than global EDPs on the retrofit effectiveness assessment by considering fragility curves. However, the EDPs choice also affects the estimates of the seismic risk, and, thus, this may significantly influence the safety level achieved through the retrofit design.

In this section, seismic risk estimates for the different retrofit levels considered are obtained by convolution of the fragility curves built using local and global EDPs with hazard curves corresponding to various hazard scenarios. In general, an hazard curve provides the mean annual frequency (MAF) of exceedance of a given value im by intensity measure IM. For $IM = PGA$, the hazard curve is described according to the form (Cornell et al. 2002):

$$v_{PGA}(pga) = P\left[PGA \geq pga \middle| 1yr\right] = k_0 \cdot pga^{-k_1} \quad (2)$$

where k_0 and k_1 are two site-dependent coefficients that are related to the hazard intensity. In this study, two different sites are considered, one with a moderate seismic hazard, and one with a quite high seismic hazard. The MAF of exceedance of 0.0021 years^{-1} (i.e., the return period of 475 years) corresponds to a PGA = 0.25g in the case of the moderate hazard, and to a PGA = 0.40g in the case of the high seismic hazard. The values of the parameters k_0 and k_1 in Eqn.2 have been obtained based on the study of Lubkowski (2010) and by following the approach reported in Tubaldi et al. (2012). They are $k_0 = $ 5.22E-5, $k_1=$ 2.67 and $k_0 = $ 9.93E-5, $k_1 = $ 3.33 respectively for the moderate and the high seismic hazard.

The hazard curves in terms of the IMs previously employed to develop the fragility curves are obtained by assuming that relation between the PGA and the IMs for a given MAF of exceedance is defined by the EC8 type 1 hazard spectrum, with soil type D ($S = 1.35$). The seismic risk for each retrofit level α, expressed in terms of MAF of system failure, v_f, has been computed as:

$$v_f(\alpha) = \int P_f(\alpha, im) \left| dv_{IM}(im) \right| \quad (3)$$

where $P_f(\alpha, im)$ denotes the fragility curve corresponding to the retrofit level α.

Figure 9 shows the values of the MAF of failure obtained by using local and global EDPs, for different retrofit levels α. and for the two different seismic hazards considered. The MAF of failure of the bare frame evaluated by using local EDPs is equal to 0.0063 yrs^{-1} and to 0.041 respectively for the moderate and high seismic hazard. This corresponds to a probability of failure in 50 yrs, $P_{f,50}$, respectively equal to 27.2% and 86.8%. The seismic risk decreases significantly for increasing α values in the range between 0.4 and 1.2, whereas it remains practically constant for α values larger than 2. These results, which are only weakly sensitive to the hazard curve considered, are in agreement with the results reported in Figure 8 plotting the capacity margin ratios.
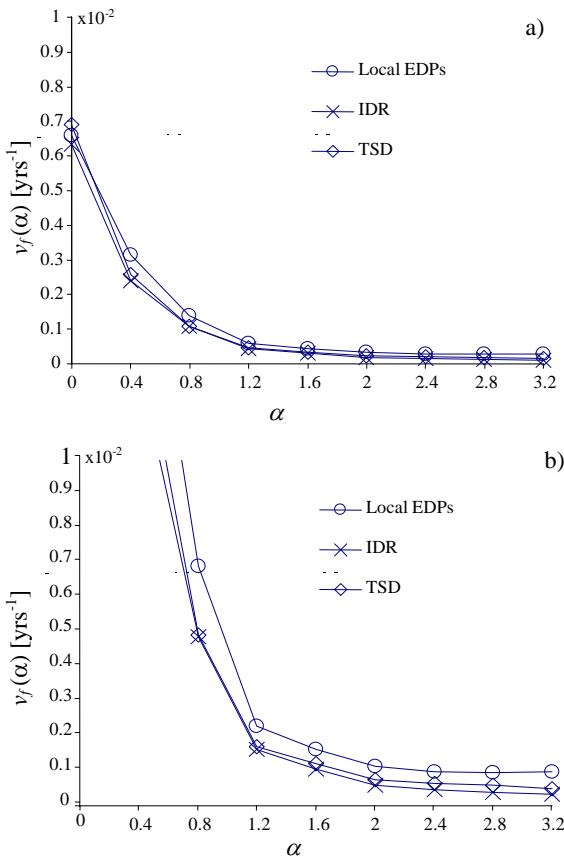

Figure 9. Seismic risks vs. retrofit level α for moderate hazard (a) and high hazard (b)

Another important result drawn from Figure 9 is that the value of the minimum risk of failure for the retrofitted system that can be achieved significantly depends on the EDPs used to build the fragility curves. Moreover, the trend of decrease is different for global and local EDPs, especially for large α values.

A target probability of failure of 2% in 50 years is assumed as retrofit objective (the corresponding value of the MAF of failure is 0.0010). The design values of α required to achieve the target failure probability obtained by using the different response parameters are reported in Table 2. In the same table, the corresponding values of the risk evaluated by using local EDPs are also reported.

Table 2. Risk-based design results.

Moderate hazard			High hazard		
EDPs	α	$P_{f,50}$	EDPs	α	$P_{f,50}$
Local	1	0.00100	Local	2.15	0.00100
IDR	0.85	0.00130	IDR	1.72	0.00140
TSD	0.85	0.00130	TSD	1.6	0.00155

In general, the use of global rather than local EDPs results in lower safety margins. In fact, for the design α levels obtained by using global EDPs a more accurate evaluation of the risk (made by using local EDPs) gives values of the risk of failure higher than that assumed as target. The differences between the design results for the different EDPs are higher in the case of high seismic hazard. For this hazard, in fact, the values of α evaluated by using TSDs and IDRs (i.e., 1.6 and 1.72) are significantly lower than the value of 2.15 obtained by using local EDPs. The corresponding values of the risk of failure are 55% and 40% higher than the target value.

6 CONCLUSIONS

This paper analyzes some aspects concerning the seismic performance assessment of existing reinforced concrete (RC) buildings with limited ductility capacity retrofitted by means of dissipative braces.

A probabilistic methodology is first introduced that permits to evaluate and compare the vulnerabilities of the frame before and after the retrofit. This methodology, similarly to other methodologies present in the literature, is based on the development of system fragility curves before and after the retrofit. However, differently from the others, it employs local rather than global EDPs to monitor the structural seismic response. This approach allows to capture accurately the modifications of the frame components' response induced by the added bracing system.

Successively, the effects of the EDPs choice on the seismic risk assessment and risk-based design of the retrofit of existing RC frames with dissipative braces is investigated by considering and analyzing a specific case study. This consists of an existing RC frame with low ductility

capacity retrofitted by inserting a system of buckling restrained braces (BRBs) with elasto-plastic behaviour. The braces are designed by applying a widespread method based on an equivalent nonlinear SDOF approximation and by considering different values of the shear capacity of the bracing system (as described by the retrofit level α).

The importance of using local EDPs in the probabilistic evaluation of the retrofit effectiveness for the type of system analyzed in this paper is demonstrated by comparing both the fragility curves and the risk estimates under different hazard scenarios. It is shown that the use of global EDPs may result in a significant overestimation of the retrofit effectiveness in terms of both vulnerability and risk reduction. Consequently, if a risk-based design is carried out for the retrofit system, the dimension of the braces evaluated by using global EDPs for vulnerability assessment are significantly lower with respect to the corresponding dimensions obtained by using local EDPs. Larger differences are observed for the hazard scenarios with higher intensity.

REFERENCES

Bracci, J.M., Reinhorn, A.M., Mander, J.B., 1995. Seismic resistance of reinforced concrete frame structures designed for gravity loads: performance of structural system. *ACI Structural Journal.* **92**(5),597-608.

Cornell, C.A., Jalayer, F., Hamburger, R., Foutch, D., 2002. Probabilistic basis for 2000 SAC federal emergency management agency steel moment frame guidelines. *ASCE Journal of Structural Engineering.***128**(4):526-32.

Dall'Asta, A., Ragni, L., Tubaldi, E., Freddi, F., 2009. Design methods for existing RC frames equipped with elasto-plastic or viscoelastic dissipative braces. *Proceedings of XIII National Conference ANIDIS.*

European Committee for Standardization (ECS). Eurocode 8 – Design of structures for earthquake resistance, EN1998, Brussels, 2005.

Freddi, F., Tubaldi, E., Ragni, L. and Dall'Asta, A. 2012. Probabilistic performance assessment of low-ductility reinforced concrete frames retrofitted with dissipative braces. *Earthquake Engineering and Structural Dynamics.* doi: 10.1002/eqe.2255

Güneyisi, E.M., Altay, G., 2008. Seismic fragility assessment of effectiveness of viscous dampers in R/C buildings under scenario earthquakes. *Structural Safety.* **30**(5),461-480.

Hueste, M.D., Bai, J.W., 2006. Seismic Retrofit of a Reinforced Concrete Flat-Slab Structure: Part II - Seismic Fragility Analysis. *Engineering Structures.* **29**(6),1178-1188.

Lubkowski Z. Deriving the seismic action for alternative return periods according to Eurocode 8. In: 14th European conference on earthquake engineering. Ohrid, Macedonia; 2010.

Katsanos, E.I., Sextos, A.G., Manolis, G.D., 2009. Selection of earthquake ground motion records: A state-of-the-art review from a structural engineering perspective. *Soil Dynamics and Earthquake Engineering.* **30**(4),157-169.

Kwon, O.S., Elnashai, A., 2006. The effect of material and ground motion uncertainty on the seismic vulnerability curves of RC structure. *Engineering Structures.* **28**(2),289-303.

Liel, A.B., Haselton, C.B., Deierlein, G.G., 2011. Seismic Collapse Safety of Reinforced Concrete Buildings: II. Comparative Assessment of Non-Ductile and Ductile Moment Frames, *Journal of Structural Engineering.* **137**(4),492-502.

Lupoi, G., Lupoi, A., Pinto, P.E., 2002. Seismic risk assessment of rc structures with the "2000 SAC/FEMA" method. *Journal of Earthquake Engineering.* **6**(4),499-512.

McKenna, F., Fenves, G.L., Scott, M.H., 2006. OpenSees: Open system for earthquake engineering simulation. Pacific Earthquake Engineering Center, University of California, Berkeley, CA.

Özel, A.E., Güneyisi, E.M., 2011. Effects of eccentric steel bracing systems on seismic fragility curves of mid-rise r/c buildings: a case study. *Structural Safety.* **33**(1),82-95.

Padgett, J.E., Des Roches, R., 2008. Methodology for the development of analytical fragility curves for retrofitted bridges. *Earthquake Engineering and Structural Dynamics.* **37**(8),1157-1174.

Ramamoorthy, S., Gardoni, P., Bracci, J., 2006. Probabilistic Demand Models and Fragility Curves for Reinforced Concrete Frames. *Journal of Structural Engineering.* **132**(10),1563-1572.

Soong, T.T., Spencer, B.F., 2002. Supplemental energy dissipation: state-of-the-art and state-of-the-practice. *Engineering Structures.* **24**(3),243-259.

Tubaldi E, Barbato M, Ghazizadeh S. A probabilistic performance-based risk assessment approach for seismic pounding with efficient application to linear systems. Structural Safety 2012; 36–37: 601–626.

Vamvatsikos, D., Cornell, C.A., 2002. Incremental dynamic analysis. *Earthquake Engineering and Structural Dynamics.* **31**(3),491-514.

Zona, A., Dall'Asta, A., 2012. Elastoplastic model for steel buckling restrained braces. *Journal of Constructional Steel Research.* **68**(1),118-125